

Multifunctional Fibers to Shape Future Biomedical Devices

Ye Zhang,* Jianxun Ding, Baowen Qi, Wei Tao, Junqing Wang, Caiyan Zhao, Huisheng Peng,* and Jinjun Shi*

Fiber-based configurations are highly desirable for wearable and implantable biomedical devices due to their unique properties, such as ultra-flexibility, weavability, minimal invasiveness, and tissue adaptability. Recent developments have focused on the fabrication of fibrous devices with multiple biomedical functions, such as noninvasively or minimally invasively monitoring of physiological signals, delivering drugs, transplanting cells, and recording and stimulating nerves. In this Review, the recent progress of these multifunctional fiber-based devices in terms of their composite materials, fabrication techniques, structural designs, device-tissue interfaces, and biomedical applications is carefully described. The remaining challenges and future directions in this emerging and exciting research field are also highlighted.

1. Introduction

Biomedical devices with 1D configuration, such as medical gauzes, surgical sutures, biopsy needles, drainage tubes, canulas, fiberscopes, and deep brain stimulation electrodes have been widely used in the clinic over recent decades.^[1,2] Advances in materials, fabrication technology, nanotechnology, and electronics have endowed these fibrous biomedical devices with entirely new functions, such as real-time monitoring physiological signals, delivering drugs, transplanting cells, and recording and stimulating nerves.^[3–5] Consequently, these multifunctional fibers prompt the development of next-generation wearable and implantable biomedical devices, which need to be miniaturized, flexible, biocompatible, and configured to make conformal contacts with human body interfaces to generate real-time medical data and provide precision medicine.^[6,7]

Dr. Y. Zhang, Dr. J. Ding, Dr. B. Qi, Dr. W. Tao, Dr. J. Wang, Dr. C. Zhao, Dr. J. Shi

Center for Nanomedicine, Brigham and Women's Hospital
Harvard Medical School
Boston, MA 02115, USA
E-mail: yzhang118@bwh.harvard.edu; jshi@bwh.harvard.edu

Dr. H. Peng
State Key Laboratory of Molecular Engineering of Polymers
Department of Macromolecular Science and Laboratory of Advanced Materials
Fudan University
Shanghai 200438, China
E-mail: penghs@fudan.edu.cn

 The ORCID identification number(s) for the author(s) of this article can be found under <https://doi.org/10.1002/adfm.201902834>.

DOI: 10.1002/adfm.201902834

1D fiber offers unique superiorities compared with 2D film and 3D bulk in both wearable and implantable applications. For wearable devices, fibers with diameters ranging from tens to hundreds of micrometers can be woven into soft, breathable, and comfortable fabrics, which could be directly used in contact with the human skin over a large area.^[8] As for implantable devices, miniaturized and flexible fibers are favorable for deep penetration into tissues^[9] through minimally invasive procedures or insertion via the natural opening, such as the gastrointestinal tracts. Moreover, these fibers can be easily retrieved and removed after the completion of sensing/therapeutic cycle. These features could drastically

reduce surgical trauma and risks of biomedical complications. In addition, the fiber structure and its small diameter provide high flexibility. They can efficiently accommodate complex deformations, well-matching biological tissues in terms of bending stiffness, and thus minimizing foreign body reaction.^[10]

In the past decade, a variety of wearable mechanical and electrochemical sensing fibers have been developed and integrated into the daily clothing to provide continuous point-of-care monitoring of breath, heart rate, and biomarkers. In the field of implantable devices, fiber-based biosensors, cell transplantation devices, and neural recording and stimulating devices have been extensively explored. These devices are designed to form a long-term stable tissue-device interface to offer prolonged close-looped diagnosis and therapy. Here, we overview the recent progress of new materials and fabrication technologies for generation of multifunctional fibers, and highlight their applications in wearable and implantable biomedical devices. We will also discuss the opportunities and challenges in this emerging yet exciting field.

2. Fabrication of Multifunctional Fibers

Developing general and sophisticated manufacturing methods for multifunctional fibers is a crucial challenge because many existed techniques, such as photolithography and nanoimprint technology, typically used for film-based devices, are not suitable for the curved surfaces of fibers. A variety of new methods including dry spinning,^[11] wet spinning,^[12] electrostatic spinning,^[13] 3D printing,^[14] microfluidic system-based spinning,^[15] and thermal drawing^[16] have been

emerged for the fabrication of fiber devices in recent decades. Various intrinsic properties, such as flexibility, biocompatibility, and conductivity, are also essential for the choice of materials. Currently, materials like conductive carbon-based nanomaterials, hydrogels, and polymers are the candidates in the extensive explorations. Below, we will introduce these three types of fibers according to the distinctive fabrication methods.

2.1. Conductive Carbon-Based Fiber

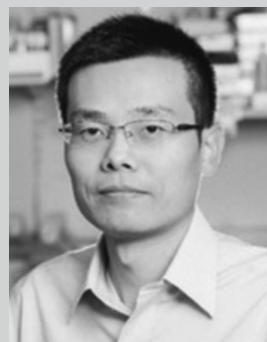
Electrically conductive fibers are highly demanded, especially for applications in electrochemical biosensors, neural recording devices, and other electronic devices. Metal, conductive polymer, and carbon-based materials are three common types of conductive substrates. Metal wires provide high electrical conductivity of 10^6 – 10^7 S m⁻¹, but they are heavy and rigid with elastic moduli of $\approx 10^2$ GPa.^[17] On the contrary, polymer fibers possess a series of merits including high flexibility, light weight, high mechanical strength, and good biocompatibility, but they suffer from intrinsic low conductivity ($< 10^4$ S m⁻¹). Coating conductive materials on the polymer fiber or introducing conductive additives during fiber spinning process may provide feasible solutions to improve their conductivity to $\approx 10^5$ S m⁻¹.^[18]

Carbon-based nanomaterials such as graphene and carbon nanotube (CNT) fibers own superior electrical and mechanical properties. Graphene is a 2D nanomaterial with a single layer of sp²-hybridized carbon atoms in a honeycomb lattice.^[19] Wet spinning technique is generally used for the preparation of graphene fibers. Briefly, a liquid crystal of graphene oxide was first injected into a coagulation bath to assemble into a continuous fiber.^[20] Graphene oxide fiber was then reduced to graphene by subsequent chemical reduction. The as-prepared graphene fiber typically showed a porous network structure, allowing the effective incorporation of guest components for producing composite fibers.^[21] Graphene fibers showed a high electrical conductivity of $\approx 10^4$ S m⁻¹, which could be further enhanced via chemical doping strategies.^[22] However, the relatively low mechanical strength of graphene fibers ($\approx 10^2$ MPa) needs to be further improved.^[23] Future research should focus on increasing the axial alignment and interlayer interaction of the constituent graphene sheets.

CNT is revealed as a single-walled or multi-walled cylindrical tube composed of sp² conjugated carbon atoms.^[24] Similar to graphene fiber, the CNT fiber can be obtained via dispersion flowing through the spinneret and coagulating in the wet bath.^[25,26] However, the low dispersibility of CNT derived from strong interactions and intrinsic chemical inertness tremendously increase the difficulty of use in spinning for the fiber preparation.^[27,28] Dry spinning is another promising technique, which exhibits advantages over traditional methods in morphology control of fiber.^[29] In the process of dry spinning, aligned CNT fiber were continuously drawn and twisted from the spinnable CNT array synthesized by chemical vapor deposition (Figure 1a,b).^[30] The entanglement and van der Waals force among the neighboring CNT bundles make CNTs forming continuous fibers.^[31] The CNTs are highly aligned along the



Ye Zhang is currently a research fellow at Harvard Medical School. She obtained her Ph.D. in macromolecular chemistry and physics from Fudan University in 2018. Her research focuses on the development of fibrous functional materials and devices for wearable and implantable biomedical applications.



Jinjun Shi is an Associate Professor of Anaesthesia at Harvard Medical School and a faculty member in the Center for Nanomedicine at Brigham and Women's Hospital. His research involves an interdisciplinary combination of biomaterials, drug delivery, nanomedicine, and immunotherapy. He has developed many multifunctional nanoparticle systems for the delivery of chemotherapeutics, proteins, vaccines, and nucleic acids, one of which has led to the first in-human clinical trial of a synthetic nanoparticle vaccine for smoking cessation and relapse prevention.

axis direction (Figure 1c). A 1.5 mm length CNT array with a width of several to tens of millimeter and height of ≈ 250 μ m can generally produce a continuous meter-long CNT fiber.^[17] The diameter within a range of several to tens of micrometer is determined by the width of CNT array and twisting speed.

The aligned CNT fibers were lightweight, flexible, mechanically strong, and electrically conductive. Electrons can rapidly hop from one CNT to adjacent ones based on the 3D hopping conduction model, which are effectively transported along the axial direction of the fiber.^[32] The CNT fibers exhibited an electrical conductivity in the range of 10^4 – 10^5 S m⁻¹ and a tensile strength up to 3 GPa.^[33] Chemical doping could be used to further enhance the electrical conductivity. The mechanical properties were improved by increasing the parallel alignment of CNT bundles and decreasing defects, and centimeter-long CNT fibers exhibit tensile strengths over 80 GPa.^[34] Bending stiffness (D) is usually used to characterize flexibility. Bending stiffness is related to diameter (d) and Young's modulus (E) of fiber, which is calculated according to the equation of $D = (\pi \times d^3 \times E) / 64$. Thus, lower Young's modulus and smaller size of fiber can reduce bending stiffness and improve flexibility. The aligned CNT fiber is flexible with low bending stiffness. Besides flexibility, stretchability is also important for the application of fiber-based materials and devices, particularly for

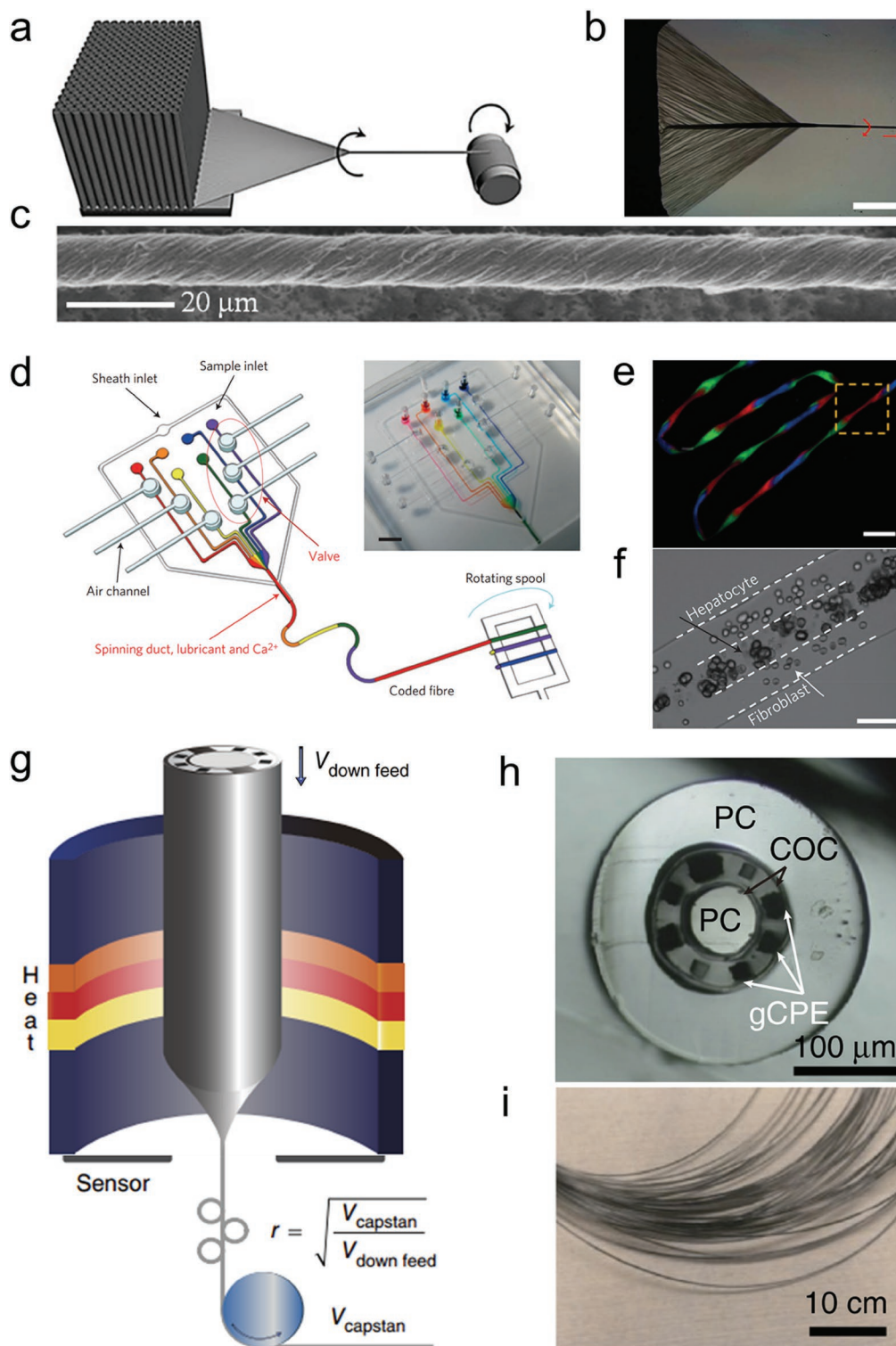


Figure 1. a–c) Fabrication methods of conductive carbon-based fiber, d–f) hydrogel fiber, and g–i) multifunctional polymer fiber. a,b) Schematic illustration and optical micrograph of the fabrication of a CNT fiber dry-spun from the aligned CNT array. Scale bars, 400 μm . c) Scanning electron microscope (SEM) image of an aligned CNT fiber. b,c) Reproduced with permission.^[30] Copyright 2012, American Chemical Society. d) Schematic illustration of the microfluidic fabrication of the hydrogel fiber. e) Fluorescence micrograph of the coded hydrogel fibers. Scale bars, 1 mm. f) Optical image of cell-containing hydrogel fiber. Scale bars, 100 μm . d–f) Reproduced with permission.^[45] Copyright 2011, Springer Nature. g) Schematic illustration of the thermal drawing process to fabricate multifunctional polymer fiber. h,i) Cross-sectional microscope image and photograph of the polymer fiber. PC, polycarbonate. COC, olefin copolymer, gCPE, conductive polymer composite comprised of conductive polyethylene and 5% graphite. g–i) Reproduced with permission.^[18] Copyright 2017, Springer Nature.

the use in vivo. By over twisting several CNT fibers together, a stretchable spring-like fiber was produced, and it showed high elongation of 305% and elasticity modulus of 9.80 MPa.^[35]

In addition to electrical and mechanical properties, biocompatibility is also an important character of CNT fibers. It was reported that short length CNTs might penetrate into living cells to interfere intracellular, whereas the CNTs in the aligned CNT fibers were hundreds of micrometers in length and assembled into aligned bundles, which were less likely to pierce through cells.^[36] In vitro experiments have shown that aligned CNTs did not trigger significant cytotoxicity for cell culturing.^[37] The aligned CNT fibers possess a high specific surface area of $\approx 10^2 \text{ m}^2 \text{ g}^{-1}$. Therefore, a variety of functional materials can be further coated onto the surface of CNT fibers to improve their physical and chemical properties by in situ synthesis, electrochemical deposition, co-spinning, and drop-casting.^[38] Due to these merits, aligned CNT fibers have been emerging in the mainstream for the fabrication of fibrous electronic biomedical devices, which will be discussed in the later section.

2.2. Hydrogel Fiber

Multifunctional hydrogel fibers are widely used for smart biomedical devices, as they can encapsulate cells, which is particularly attractive for tissue engineering and cell transplantation applications. These fibers are generally fabricated in vitro to mimic the intrinsic morphologies and functions of human tissues, such as muscle fibers, blood vessels, liver, pancreatic islets, and neural networks. The preparation of cell-containing fibers requires the use of biocompatible and nontoxic materials under mild conditions.

The hydrogel is a highly water-absorbent 3D polymer network,^[39] with a similar structure to extracellular matrices of natural tissues, thus allowing cells to proliferate and grow. Alginate, supramolecular hydrogels, chemically modified gelatin, and photo-crosslinkable methacrylate gelatin are most widely used materials to prepare hydrogel fiber.^[40] As a Food and Drug Administration (FDA)-approved biomaterial, alginate is the most popular hydrogel matrix due to its superior biocompatibility, low toxicity, relatively low cost, high mechanical property, and mild preparation conditions.^[41]

Continuous hydrogel fibers are often fabricated by wet spinning technique^[42] through the injection of the precursor solution into a coagulation bath. For example, after injecting a solution of sodium alginate into a solution of calcium chloride (CaCl_2), it was crosslinked rapidly by exchange of Na^+ and Ca^{2+} to form the fibrous hydrogel network. The diameters of the fibers were controlled by the diameter of the needle and the rate of injection, which can be as small as tens of micrometers.

Microfluidic spinning offers precise control over the morphology, size, and chemical composition of the hydrogel fibers^[43] with the similar mechanism of operation to that of wet spinning. However, there are two or more streams of coaxial flowing in microfluidic channels compared to the single mode of wet spinning.^[44] Hydrogel fibers were produced by solidifying the inner flow through ion crosslinking or photopolymerization processes. As shown in Figure 1d, a typical microfluidic spinning chip was comprised of some individually controllable

inlets.^[45] Six different sodium alginate solutions were flowed through the independent microfluidic channels. A digital fluid controller precisely controlled the fluid volume of each channel. At the end of the chip, a coaxial flow was generated with CaCl_2 solution as the sheath and mixed sodium alginate solution as the core. The ion exchange between CaCl_2 flow and alginate flow induced subsequent rapid gelation, resulting in an alginate fiber formation. By regulating the fluid flow of each channel, hydrogel fibers can be obtained with diverse chemical compositions, gas bubbles, morphologies, and structures (Figure 1e). Single or co-cultured live cells can also be encapsulated in the fibers. As shown in Figure 1f, the primary rat fibroblasts and hepatocytes were co-cultured and coded in parallel along the length of the fiber. The viability of hepatocytes was maintained up to 5 days.

The activity and function of cells were further enhanced in the natural extracellular matrices (ECM) proteins-tethered hydrogel fibers, which allows cells migrating in three dimensions and connecting to each other. However, the microfluidic technique required gelation of solutions in a short time scale of less than 1 s, thus making it not directly applicable for natural ECM proteins which need a much longer gelation time. To solve this issue, a double-coaxial laminar flow microfluidic technology was developed to fabricate core-sheath hydrogel fibers with cell-containing ECM proteins in the pre-gel state as a core and mechanically stable alginate hydrogel as a shell.^[46] The alginate hydrogel shell prevents the proteins diffusing away from the core, and the proteins thus have sufficient time to be gelated. The cells in the core were cultured to form a fibrous cellular structure, while the ECM proteins provided a suitable microenvironment for cell migrations and proliferations. The alginate shell can also be removed to develop hydrogel fibers only comprising of cells and proteins. This method extends the application of microfluidic technology to various materials. In addition, the multichannel coaxial extrusion system of the microfluidic device can be also used to fabricate hollow tubes aiming to imitate human cannular tissues, such as blood vessel.^[15]

2.3. Multifunctional Polymer Fiber

Multifunctional polymer fibers have been developed as effective tools in neuroscience and neuroprosthetics.^[47] These fibers with diameters of tens of micrometers are required to have as many electrodes as possible with different functions. Thermal drawing technology, which is traditionally employed in optical fiber production, has been explored as an appropriate method to produce multifunctional polymer fibers.^[4,48] In this process, a multi-material cylindrical or cuboid preform with complex section structure is first fabricated by macroscale machining. This preform has the same geometry and composition as the final fiber, but with much larger cross-sectional features and shorter lengths. The preform is then heated and stretched into a fiber with a well-maintained geometry, reduced cross-sectional dimension, and increased length up to kilometers.^[49,50]

The key to this preparation process is to ensure that materials can be co-drawn and to prevent axial and cross-sectional capillary break-up. Therefore, several conditions of materials

should be carefully taken into considerations. First, the materials possess similar glass transition and melting temperatures. Second, the materials possess sufficiently low viscosities ($<10^7$ Poise) at the drawing temperature, allowing for continuous and simultaneous flow. Finally, the materials exhibit good adhesion in the viscous and solid states without breaking even under a rapid cooling process.

Figure 1g shows a typical polymer fiber production process by thermal drawing at 240 °C using a fiber drawing tower.^[18] The fiber with a diameter of ≈ 200 μm was composed of an optical waveguide for neural stimulation, six conductive electrodes for neural recording, and two microfluidic channels for the drug delivery to the specific site (Figure 1h). In the optical waveguide part, polycarbonate and cyclic olefin copolymer exhibit low absorption in the visible spectrum, while the difference between their refractive indexes permits light confinement within polycarbonate. Because the glass transition and melting temperatures of polycarbonate, cyclic olefin copolymer, and conductive polyethylene are in an identical range, they can be thermally drawn simultaneously. The obtained multifunctional polymer fiber was highly flexible with bending stiffness of 76.1–83.5 N m^{-1} (Figure 1i). The thermal drawing method has the unique superiority of enabling complex and multiple functionalities within fibers, whereas this method is limited in the materials' compatibility and the requirement of extremely high heating temperatures.

3. Wearable Devices

The development of wearable biomedical devices for noninvasive automated personalized healthcare is a fast-growing multidisciplinary research area. These devices are expected to be worn conformably on the human body for sensing^[51] electrophysiological and biochemical signals, or delivering drugs,^[52] which are very useful for patients in detecting diseases at an early stage, treating disease in an intelligent closed-loop way, and reducing healthcare expense by timely prediction and prevention of disease.^[53] In order to integrate wearable devices on the human body and negate any inconvenience, these devices are indispensably required to be lightweight, flexible, and stretchable, as well as comfortable and reliable of wearing. Also, the devices have to cover irregular and dynamic surfaces such as human body and bear a variety of deformations. As an ideal platform for wearable devices, fiber-based textiles have been used for thousands of years due to the unique features of softness, flexibility, air permeability, and durability.^[3] Therefore, a variety of novel fiber-shaped biomedical devices have been developed and seamlessly integrated into fabrics or daily clothes while maintaining their advanced properties.

3.1. Wearable Sensor

Wearable sensing fibers are often designed to gather and convert biomechanical activities and physiological signals to another suitable form such as electrical signals. Then, the signals are transmitted to the remote center by wireless communication for further processing, aiming to achieve continuous

and long-term tracking of the wearer's health state.^[54,55] Therefore, these sensing fibers are required to possess appropriate measurement range, high sensitivity, ultra-fast response, and recovery rate for real-time monitoring.

Sensors responding to mechanical force including pressure, strain, tension, and shearing forces have been extensively explored for a variety of applications including monitoring patients, caring for the elders, and detecting human motions.^[56] For example, continuous monitoring of heartbeat traces significantly revealed early stages of heart diseases. Detecting human movements provided valuable information for clinical rehabilitation. Sensors responding to mechanical signals are classified as resistive, capacitive, piezoelectric, and triboelectric sensors according to their different sensing mechanisms.

Resistive sensors^[57] typically consist of a conductive fiber that change their geometries with a resistance change in response to an applied force. These fibers are usually fabricated by the incorporation of conductive CNTs,^[58] silver nanoparticles, or nanowires^[59] into elastic polymer fibers. Applied force leads to disconnection among conducting materials or crack propagation and, consequently, changes the electrical resistance.^[60] They can detect a broad range of pressure and strain, but most resistive sensors suffer from poor sensitivity and cannot detect low mechanical stimulations.^[56] Capacitive sensors^[61] are generally fabricated by using two conductive layers as electrodes, which are separated by dielectric spacers. Upon application of a force of deformation, the change of thickness leads to capacitance variation. The capacitive sensors are also suitable for large strain monitoring. These sensors are usually assembled onto clothes, gloves, and stockings, to detect different types of human motions such as walking, breathing, speech, and emotional expressions.^[62]

Piezoelectric sensors can convert mechanical stimulations to electric signals based on the piezoelectric effect.^[63] Piezoelectric sensors usually use ZnO nanowires^[64] or poly(vinylidene fluoride)^[65] as the active piezoelectric material, which demonstrates advantages of fast response, high sensitivity, and self-power. Triboelectric sensors^[66] transform mechanical signals into electric signals based on a coupled effect of electrostatic induction and contact electrification. A typical example is shown in Figure 2a.^[67] A silver-coated nylon fiber was used as electrode, while silicone rubber with a strong tendency to gain electrons was chosen as the dielectric. The conductive fibers were woven into a continuous and interlaced network and then uniformly distributed in the silicone rubber elastomer. The schematic of the operation mechanism is shown in Figure 2b. When the skin contacts to silicone rubber, electrification occurs and the same amounts of charges with opposite polarities are generated at the surface of the skin and the silicone rubber, respectively. Once the skin moving away, positive charges transfer from the skin to the inner fiber electrode due to the electrostatic induction effect. The accumulated different potentials between the skin and the inner fiber electrode prompt electrons to flow, thereafter generating an instantaneous current. Its electrical current and potential outputs were found to approximately linearly increase with the increasing loading forces. Due to the high sensitivity in pressure, the triboelectric sensors are able to detect arterial pulse waves (Figure 2c).

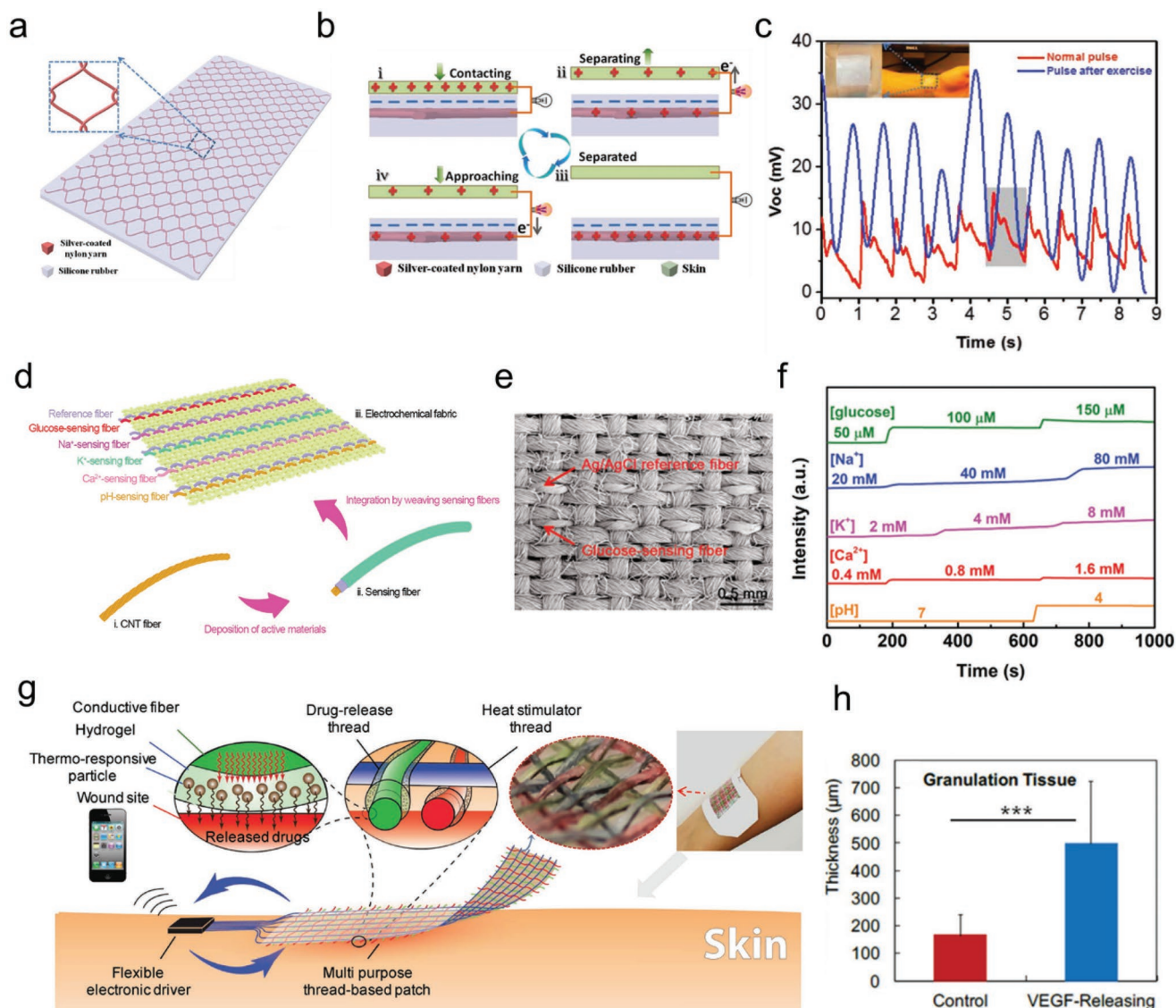


Figure 2. Wearable fiber-based biomedical devices. a) Schematic illustration of the triboelectric sensing textile with "chain-link" fence-shaped structure and rhombic unit design. b) Schematic of the operation mechanism of the triboelectric sensing textile. c) Real-time arterial pulse waves under normal and exercise conditions. Inset is the photograph of a sensing textile attached on a wrist. a–c) Reproduced with permission.^[67] Copyright 2018, Wiley-VCH. d) Schematic illustration of the fabrication of electrochemical fabric by weaving sensing fibers, and these fibers were made by depositing active materials on CNT fiber substrates. e) SEM image of a textile containing glucose-sensing fibers and Ag/AgCl reference fibers. f) System-level interference studies of the sensing fibers in electrochemical textile. d–f) Reproduced with permission.^[70] Copyright 2018, Wiley-VCH. g) Schematics of a multipurpose fiber-based patch for transdermal drug delivery. The fibers which were consisted of a conductive fiber heater as core and a hydrogel layer carrying thermoresponsive particles as sheath, were assembled into fabrics and connected to a microcontroller that would individually power them up. h) Results of measurements of granulation tissue deposition. g,h) Reproduced with permission.^[73] Copyright 2017, Wiley-VCH.

In addition to physical signals, monitoring health state at molecular levels is also essential,^[68] e.g., sweat contains rich physiological and metabolic information. The concentration of sweat electrolyte and pH value are important indicators for detecting electrolyte loss and dehydration during exercise.^[69] Accordingly, a variety of sensing fibers have been explored for real-time monitoring of physiological signals (e.g., pH, glucose, Na⁺, K⁺, and Ca²⁺) in sweat.^[70] Figure 2d shows an integrated electrochemical textile as a wearable platform where CNT fiber was used as a conductive skeleton to load different kinds of active materials. The pH-sensing fiber was fabricated

by electrodepositing polyaniline onto the surface of CNT fiber. The CNT/polyaniline hybrid fiber served as the working electrode, while the Ag/AgCl fiber was used as the reference electrode. At different pH values, the change of polyaniline surface protonation led to different zeta potentials of the hybrid fiber. For glucose-sensing fiber, a layer of Prussian blue was first electrodeposited on the CNT fiber as a mediator to provide better sensitivity. Thereafter, a permeable chitosan film containing glucose oxidase was coated as the active layer. The ion-sensing fibers were fabricated by coating especially ion-selective ionophore and poly(3,4-ethylenedioxythiophene):poly(styrene

sulfonate) onto CNT fiber. These different kinds of sensing fibers were finally woven into a flexible integrated textile to monitor sweat metabolites (Figure 2e). It should be noted that high sensitivity is required for accurate monitoring because the concentrations of many biomarkers are much lower than those in blood. Besides, the reliability and signal stability of fibrous electrochemical sensors need to be further improved.

3.2. Drug Delivery

Besides real-time monitoring, a feedback therapeutic system is also highly required to improve the quality of treatment and healthcare management, especially for chronic diseases.^[71,72] For example, chronic ulcers and wounds are major biomedical challenges for the patients with diabetes or varicose veins. Due to the lack of system for the delivery of relevant biological factors, chronic wounds remain at the inflammatory phase, which impairs re-epithelialization and healing. Developing a wound dressing that can achieve real-time monitoring and controllably deliver various therapeutic factors at different stages would be beneficial for effective treatments of chronic wounds.^[73] As shown in Figure 2g, a multi-purpose fiber-based patch was developed for transdermal drug delivery. The cotton thread was coated with a layer of conductive carbon ink and subsequently covered with a hydrogel layer containing thermo-responsive microparticles as drug carriers. These particles could be used for the encapsulation of various antibiotics and growth factors. The fibers loaded with different drugs were woven into a flexible textile where each fiber was individually operated as an independent functional unit to enable the on-demand release of a specific drug. The textile was further connected to a microcontroller to transfer commands from smartphone wirelessly. The fiber-based textile was tested in a diabetic wound mice model *in vivo*. Histology and wound closure studies confirmed the effectiveness of the proposed smart textile on improving healing rate (Figure 2h). In addition to thermal stimulation, light stimulation can also trigger the release of drugs in the fibers.^[74] It should be noted that a fabric consists of thousands of fibers. Therefore, different kinds of fiber devices including sensing fibers with different functions, drug delivery fibers, energy supply fibers, signal transduction fibers, and wireless transmission systems should be integrated into a textile. Future work should focus on developing fully integrated multiplexed sensing and therapeutic textiles to achieve remote real-time monitoring for closed-loop treatment.

4. Implantable Devices

Compared to wearable biomedical devices, implantable devices provide more *in vivo* physiological relevant information for medical diagnosis, prognosis, and therapies.^[75–77] These devices are required to induce minimal tissue damages, form long-term stable interfaces, capture biomarkers with high efficiency, record physiological signals with high signal-to-noise ratios, and deliver drugs with pinpoint spatial accuracy.

To meet these requirements, a variety of fiber-based implantable devices have been widely investigated. These devices are

fabricated by thin and flexible fibers with diameters of tens of micrometers, where the 1D configuration of fiber makes it available to be directly implanted into tissues with minimal invasiveness. Compared to conventional surgical implantation, it effectively helps patients to get rid of the risks of inflammation and reduces recovery time and medical care. Moreover, the high flexibility and small size at micrometers in diameter of implantable fiber results in less debris and rapid recovery of the tissues.

4.1. Biosensor

Many wearable sensors tested *in vitro* are being developed into implantable devices to analyze biological and physical signals in the brain, blood, tumor, and other tissues. For example, accurate analysis of ascorbic acid levels in the active brain has diagnostic values and potentially therapeutic functions for neurodegenerative diseases. Aligned CNT fibers with engineered tunable defects and oxygen-containing species were used as electrodes for the accurate detection of ascorbic acid concentration in live rat brains.^[78] O₂ and pH values are important species correlated with brain ischemia and cancer growth. Based on a similar strategy, an electrochemical sensing CNT fiber was also developed (Figure 3a).^[79] Hemin-Fc as active material was attached onto the CNT fiber through π - π stacking interactions. As shown in Figure 3b, the reduction peak current of hemin gradually increased as function of increasing O₂ concentration, resulted from the electrocatalytic activity of hemin. It converts O₂ to H₂O through an electrochemical reaction, followed by a chemical reaction with one electron and one proton, leading to the determination of O₂ concentration with a linear range of 1–200 × 10⁻⁶ M. Meanwhile, as demonstrated in Figure 3c, the peak potential shifted positively in accordance with decreasing pH, allowing determination of pH values with good linearity from 5.5 to 8.0. Therefore, the biosensor fiber for the simultaneous accurate quantification of O₂ and pH using both outputs of current and potential signal was achieved. The fiber sensor with a diameter of ≈10 μm was also successfully applied in live mouse brains with ischemia, as well as in tumor during cancer starvation therapy to verify the validity *in vivo*.

Electrochemical sensing fibers have achieved high detection accuracy but suffer from signal drift due to the instability of electrochemical reactions *in vivo*. Hydrogel optical fibers are a promising alternative for continuous and long-term quantifiable monitoring due to their high biocompatibility and ability to incorporate functional materials for sensing.^[68,80] For instance, flexible hydrogel optical fibers were fabricated with poly (acrylamide-co-(poly (ethylene glycol) diacrylate)) as the core and a Ca²⁺ alginate cladding for quantitative glucose measurements. 3-(acrylamido)-phenylboronic acid molecule was covalently incorporated into the core, which can change the physical and optical properties in response to glucose.^[81] Hydrogel optical fibers can be inserted subcutaneously for quantitative monitoring of glucose concentration in interstitial fluid by measuring the changes in the intensity of transmitted light through the hydrogel optical fiber.

Apart from continuous analysis of physiological signals *in vivo*, fiber devices were implanted in blood vessels to retrieve

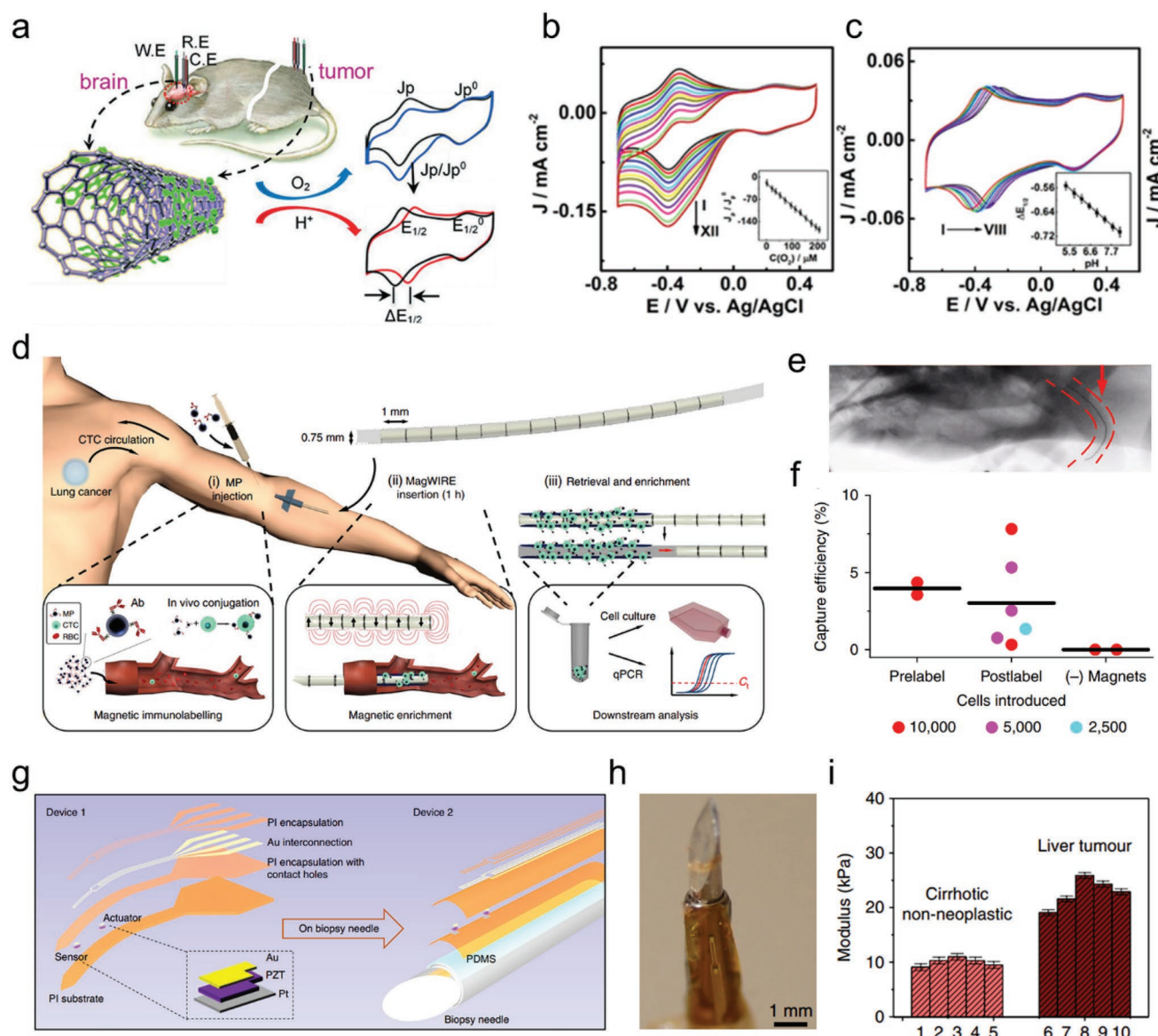


Figure 3. Implanted biosensing fibers. a) Illustration of the working mechanism of the electrochemical sensing fiber for simultaneous determination of O_2 and pH. b) Cyclic voltammograms obtained from the Hemin-Fc/CNT sensing fiber in 0.1 M PBS bubbled with different O_2 concentrations. c) Cyclic voltammograms obtained at Hemin-Fc/CNT sensing fiber in 0.1 M phosphate-buffered saline (PBS) (N_2 -saturated) with different pH values. a–c) Reproduced with permission.^[79] Copyright 2017, Wiley-VCH. d) Schematic of the concept of intravascular magnetic wire for high-throughput retrieval of circulating tumor cells in vivo. e) Fluoroscopy of the flexible magnetic wire (red arrow) advancing through a tortuous vessel in a porcine model. f) Cell-capturing efficiencies in the porcine model. g–i) Reproduced with permission.^[82] Copyright 2018, Springer Nature. g) Schematic illustrations of the needle-shaped ultrathin piezoelectric microsystem (device 1) integrated on a biopsy needle (device 2). PZT, lead zirconate titanate; PDMS, polydimethylsiloxane; PI, polyimide. h) Photograph of the sensor and actuator regions on the biopsy needle substrate. i) Modulus values obtained from healthy and cancerous tissues. g–i) Reproduced with permission.^[83] Copyright 2018, Springer Nature.

rare biomarkers with high yields.^[82] The detection and analysis of rare blood biomarkers are extremely necessary for early diagnosis of disease. However, some biomarkers such as circulating tumor cells are inadequate for isolation and analysis in a 5–10 mL blood sample. Multifunctional fibers can solve this problem in a new way. As shown in Figure 3d, a flexible magnetic fiber was used for intravascular retrieval and enrichment of circulating tumor cells. Due to the advantages of small dimension, flexibility, and the plastic sheath's biocompatibility, the self-contained magnetic fiber was easily inserted into a superficial

blood vessel through a standard intravenous catheter (Figure 3e). Antibody-coated magnetic particles were injected into the blood to label the circulating tumor cells. As the entire blood volume circulated past, the labeled cells were captured and enriched on the magnetic fiber. The fiber was then retrieved to elute the targets for downstream analysis. As the fiber can capture labeled biomarkers from the subject's entire blood volume, the capture efficiency is improved by 10–80 times compared with a 5 mL blood draw (Figure 3f). This method can be extended to capture other rare biomarkers in circulating blood as well.

Analyzing physical signals is also important, and mechanical measurements in the organ tissues provides a significant diagnostic basis for assessing patient health and disease progression. For example, distinctive elastic moduli are shown in the normal tissues and cancer tissues. Thus, minimally invasive measurements of mechanical properties can be used to distinguish and target diseased tissues with a high accuracy. As shown in Figure 3g, a needle-shaped mechanical sensor was developed to accurately target a tumor site during biopsy procedures through quantitative measurements of variations in tissue modulus.^[83] The device contained two separate micro piezoelectric assemblies to provide mechanical sensing and actuation. The contacting modulus of tissue can be measured by analyzing data from the induced voltage of the sensor after applying a voltage to the actuator. The sensor was built on a thin, flexible, and free-standing polyimide substrate with a sharp tip geometry and narrow width, which can directly penetrate through the targeted tissues or install onto conventional

biopsy needles (Figure 3h) to quantitatively measure tissue moduli (Figure 3i). Future work should focus on the development of multifunctional integrated fibers that enables more clinical-orientated monitoring.

4.2. Cell Transplantation

The fiber-based strategy is also attractive for cell transplantation to provide artificial tissue replacements for patients suffering from tissue failure. Fiber-containing living cells could be useful for the treatment of hormone deficient diseases and endocrine disorders, such as diabetes mellitus.^[84] In these cases, hydrogel fibers are usually used to transport cells to the desired site and control the function and structure of the artificial tissue. As shown in Figure 4a,b, the fiber could be extended to meters in length. They were in a coaxial configuration with glucose-responsive insulin-secreting pancreatic islet cell as the

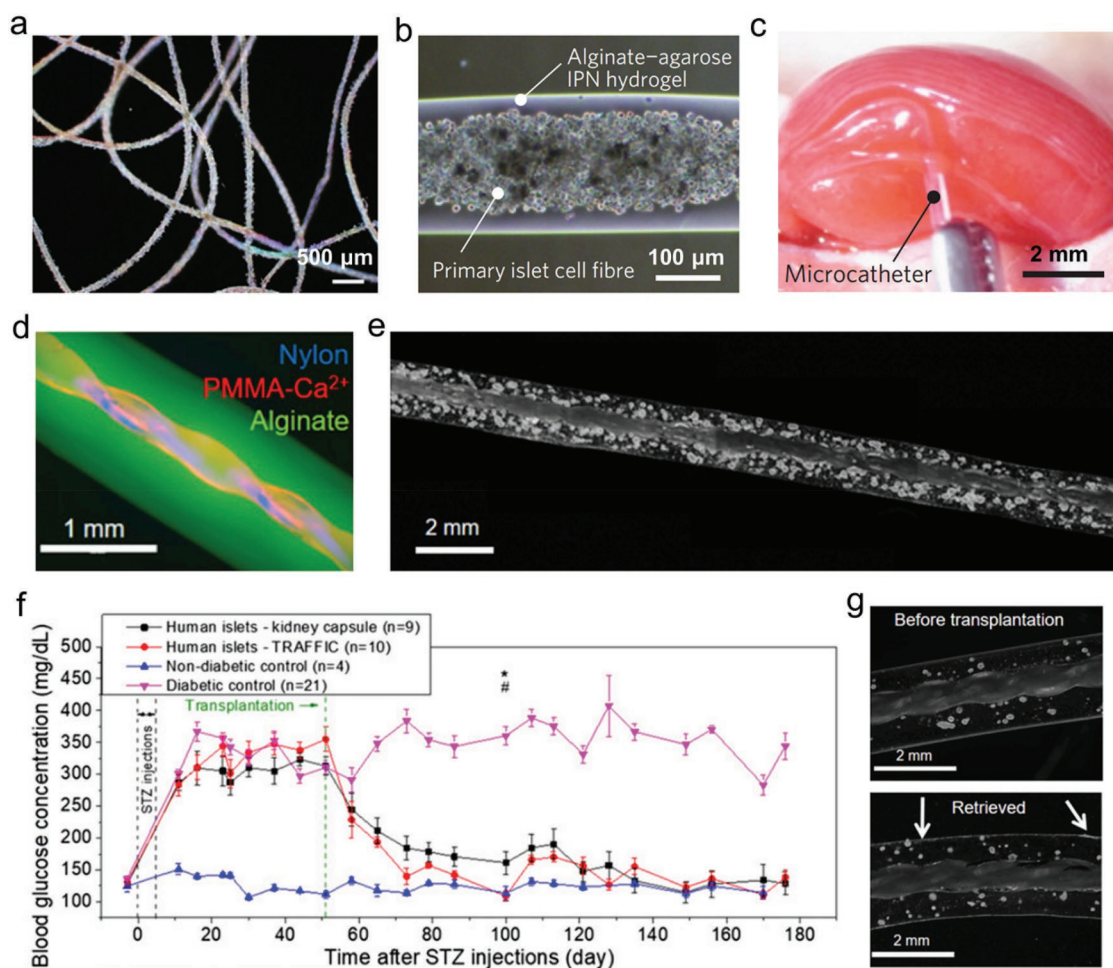


Figure 4. Cell-containing hydrogel fiber for cell transplantation. a) Optical image of the meter-long cell-laden microfiber. b) Optical image of a primary islet cell fiber with an alginate–agarose interpenetrating network hydrogel shell. c) Photograph of the implantation of a 20 cm long primary islet cell fiber into the subrenal capsular space of a recipient mouse during the implantation. a–c) Reproduced with permission.^[46] Copyright 2013, Springer Nature. d) Fluorescent micrograph of the reinforced polymer/alginate hydrogel hybrid fiber encapsulating islet cells. e) Microscopic image of the reinforced polymer/alginate hydrogel hybrid fiber. f) Blood glucose concentrations of diabetic mice after transplantation of hybrid fiber with encapsulated islet cells. g) Microscopic images of the hybrid fiber with encapsulated islet cells before and after transplantation in dogs (the arrow points to the minimal cellular overgrowth on the fiber). d–g) Reproduced with permission.^[85] Copyright 2018, National Academy of Sciences.

core, while alginate–agarose interpenetrating hydrogel as the shell.^[46] The encapsulated hydrogel shell was able to isolate the fiber from fibrotic reaction caused by the host response. It also protected the cells in the core from immunological attack and simultaneously allowed mass transfer to maintain cell function. The 20 cm long cell fiber containing approximately 0.6×10^6 cells was injected and folded into the sub-renal capsular space of a diabetic mouse by a microcatheter (Figure 4c). The unique 1D shape and small size enabled these cell fibers to be highly compatible with minimally invasive procedures, such as catheter intervention. The blood glucose concentrations were confirmed to be normal for 13 days. This work is marked as a significant advance in the field of *in vivo* tissue reconstructions.

However, the mechanical strengths of these hydrogel fibers are relatively low. Optimal mechanical properties are particularly desirable because the fibers are intentionally designed for the long-term *in vivo* use with a retractable character after completion of therapy. Therefore, robust polymer fibers were introduced as a core to improve their mechanical properties. Hydrogel seeded with living cells were coated or *in situ* cross-linked within the polymer fibers. Compared with bare alginate hydrogel fiber, the hybrid fiber exhibited drastically higher strengths and *in situ* cross-linking guaranteed the tight adhesion between the polymer fibers and the hydrogels.^[85] The hydrogel layer formed around the fiber was uniform (Figure 4d), enabling that rat islets cells were encapsulated in the shell layer (Figure 4e). After *in vivo* transplantation, the blood glucose levels were maintained within the normal range for more than 4 months (Figure 4f). Besides, after 1 month of implantation in dogs, the fiber can be entirely retrieved through a minimally invasive laparoscopic procedure (Figure 4g). The unique removable feature of hydrogel fiber is more beneficial compared to other cell encapsulating methods, such as hydrogel microcapsules,^[86,87] which can reduce risks in the event of medical complications or transplant failures, and therefore improve therapeutic safety in a satisfactory level.

4.3. Neuroengineering

Multifunctional fibers are urgently needed in both neuroscience research and neuroprosthetics, in order to record neural activities at a single neuron resolution and communicate with neurons across diverse signal modalities. Thus, these devices have great potentials to treat psychiatric and neurological disorders or to restore functions followed by nerve injury.^[88,89]

Implantable neural fibers to record extracellular potentials from targeted neurons have been extensively investigated for clinical neuroprosthetic researches.^[89] These fibers are required to record neural activity from the same neurons for a long-term frame with high fidelities and reliabilities. Therefore, neural recording fibers should have a small size (diameter $<50 \mu\text{m}$) comparable to individual neurons, which is in a good match with mechanical properties of single neurons to reduce the damage to the local neuronal environment. They should also be able to minimize perpetual mechanical trauma caused by physiological motion between the fibers and the surrounding tissues. Moreover, neural recording fibers should demonstrate high charge injection capacity and low electrical resistivity

and impedance to enable high signal-to-noise ratios for neural recording.

Carbon-based fiber materials, such as carbon fiber, CNT fiber, and graphene fiber, provide both high electrochemical properties, stability, and flexibility, making them as ideal materials for neural recording. As shown in Figure 5a, a thin fiber was developed with a $7 \mu\text{m}$ diameter carbon fiber as the core, a poly(*p*-xylylene)-based thin-film coating as a dielectric barrier, a thin layer of poly(ethylene glycol) as a biofouling-resistant surface, and a polythiophene-based recording pad on the tip of the neuronal fiber.^[10] As a result, the fiber showed a bending stiffness of 4540 N m^{-1} , which was more mechanically compliant with brain tissues than traditional silicon recording electrodes. They were found to reduce chronic reactive tissue responses and enabled single-neuron recording in acute and early chronic animal models. Initial chronic neural recording studies suggested that these microelectrodes were stable for over 5 weeks in the brain (Figure 5b). CNT and graphene fibers attract increasing attentions with another promising advantage of high specific surface areas in comparison with carbon fiber.^[90,91] The porous structure and thin-layer conductive coating can further improve the surface area and reduce the electrical impedance, which results in a large charge injection capacity and a high recording sensitivity.^[90]

The neural recording fibers were further developed into multifunctional fibers for simultaneous optical stimulation, chemical stimulation, drug delivery, and neural recording. For example, a multifunctional neural fiber was fabricated by the thermal drawing process, which incorporated a cylindrical waveguide, two microfluidic channels, and two recording electrodes (Figure 5c).^[92] The integrated polymer fibers were suitable for combined long-term optogenetic and pharmacological interrogation and neural recording in freely moving mice (Figure 5d,e). In addition, the multifunctional fibers were also used for local drug administration for neurodegenerative disorders. Systemic drug administration results in broad drug distribution and thus increases the risk of toxicity. Local drug administration into affected brain areas reduces risk, but the amount and target site of the drug should be accurately controlled to minimize drug diffusion and leakage. A miniaturized neural drug delivery fiber with a diameter of $200 \mu\text{m}$ and an aspect ratio of ≈ 500 was developed (Figure 5f,g).^[93] It was integrated with a tungsten electrode to record neural activity for a potential feedback control at the single-cell and population level, and two fluidic channels connected to modified wireless pumps delivered nanoliters of drugs on demand. It was effective for at least 2 months' test in rats and nonhuman primate, which demonstrated chronic behavioral and acute electrophysiological effects (Figure 5h).

5. Challenges and Outlook

Over the past few decades, advances in materials and devices manufacturing technology have accelerated the development of multifunctional fibers in the realm of biomedicine. These new devices have been demonstrated to have immense potentials, which will expand the ranges of diagnostic and therapeutic technologies. Although significant progresses have been

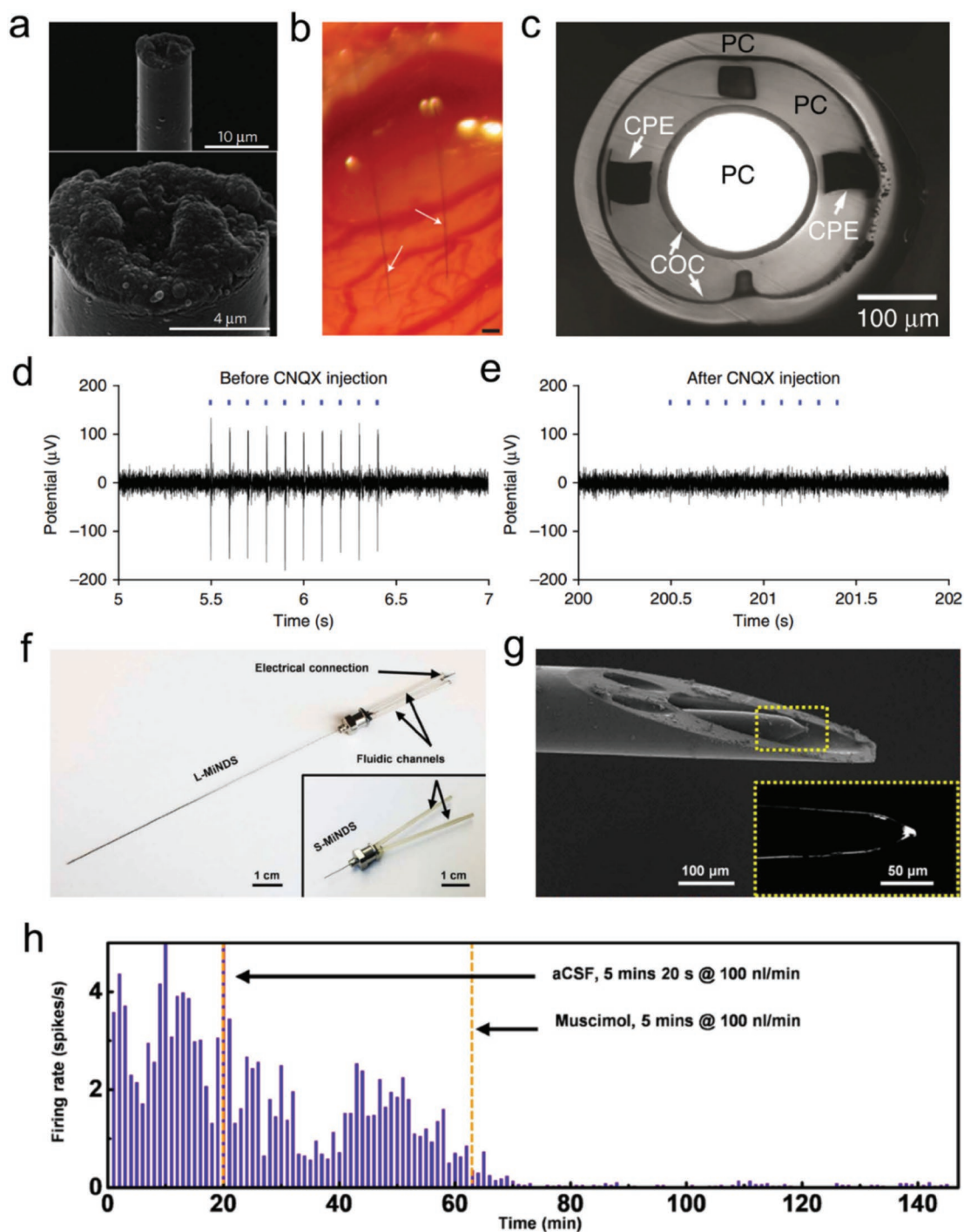


Figure 5. Fibers for neuroengineering. a) SEM images of the neural recording fiber. b) Neural recording fibers (arrows) implanted 1.6 mm deep into the cortex. Scale bar, 100 μm . a,b) Reproduced with permission.^[10] Copyright 2012, Springer Nature. c) Cross-sectional optical image of the multimodality polymer fiber for combined optogenetic and pharmacological interrogation and neural recording. d,e) Electrophysiological recording by multimodality fiber before and after injection of drug during optogenetic stimulation (10 Hz) for 20 s, respectively. c–e) Reproduced with permission.^[92] Copyright 2015, Springer Nature. f) Photograph of miniaturized neural drug delivery fibers. g) SEM images of the tip of the drug delivery fiber. h) In vivo modulating and monitoring local neuronal activity in the neocortex of a nonhuman primate through serial infusions of artificial cerebrospinal fluid and muscimol. f–h) Reproduced with permission.^[93] Copyright 2018, American Association for the Advancement of Science.

achieved, this field still remains at proof-of-concept and several challenges need to be overcome before we can take full use of multifunctional fibers in biomedical applications.

The biocompatibility and biosafety of fibrous devices should be meticulously considered and strictly evaluated. It has been reported that cells-containing hydrogel fiber may induce

variable cellular overgrowth after several months' implantations.^[85] The choice of materials considering the biocompatibility with matching size and stiffness is an important factor to avoid foreign body reactions. For example, the neural probes which matched the subcellular feature sizes and mechanical properties of neurons were reported to form stable interfaces with the neuronal and glial networks. The probes elicited negligible immune response and demonstrated stable single-unit recording without loss in recording quality for at least 3 months.^[94] More comprehensive biosafety experiments, such as long-term toxicity analysis, are particularly required for invasive applications. In addition, wearable devices are closely in contact with skin, and it is thus necessary to improve their adaptability toward skin and critically assess the electromagnetic radiation from wearable devices.

Accuracy and reliability are crucial for practical clinical applications of sensing and recording devices. Especially for implanted devices, the accuracy loss is more serious, which is mainly caused by foreign-body responses including inflammatory reaction and fibrosis, surface fouling deposition, and instability of electrochemical reactions. Improvement of biocompatibility and effective strategies of surface modifications can mitigate acute inflammation and reduce signal noise. Moreover, the coating materials of sensors can also minimize biofouling effects, which should be carefully taken into consideration. As for neural recording fibers, the neuronal loss and glial scar formation around the implantation sites result in signal degradation.^[94] For long-term and accrual recording of neural activity, future work should focus on developing thin cross-sectional and mechanically matching neural fibers to reduce damages of the local neuronal environment, and minimize mechanical trauma caused by physiological motion.

Integrating more functions into a fiber or fiber-based textile is a future trend in biomedical devices. Current fiber-based wearable and implantable devices contain no more than ten sensors and drug delivery channels, far from meeting the demands. On the one hand, more fibrous sensors should be developed for detecting a wide range of physiological signals. On the other hand, fibrous biomedical devices, as a new and multidisciplinary field, are expected to fuse with new strategies of treatment such as photodynamic, immunological, and regenerative therapy. Fibrous devices can achieve integration by ingenious structure design. Hundreds of components with different functions may be connected in series along the axial direction or co-drawn in parallel with the axial direction. Sensing and therapy components can also be designed in a core-sheath structure to achieve closed-loop treatment. Moreover, more efforts should be exerted to exploit generalizable and efficient weaving methods aiming at integrating these devices with different functions into textiles or daily clothing for wearable devices.

Other components such as power supply, wireless transmission, and data analysis are also crucial for the practical utility of these fibrous biomedical devices. A variety of flexible and stretchable fibrous lithium-ion batteries has been developed and woven into textile to supply power into wearable sensors.^[95,96] Energy harvesting and storage devices, including biofuel cells, piezoelectric and triboelectric generators, supercapacitors and aqueous batteries, have been used in vivo as

implanted devices.^[97] Researchers need to further improve the energy density and safety for long-term power supply to prolong the service time of implanted biomedical devices and reduce the risks and pains of replacement. Data analysis is a huge challenge because of large amounts of data generated by real-time detection. Thus, large data processing technologies, machine learning, and artificial intelligence will be introduced to analyze the complex data in order to provide the biological and clinical advices. The understanding of the clinical relevance of the sensor data also needs further progress. Finally, from an engineering viewpoint, future research should focus on the development of large-scale production facilities and effective fabrication methods to transform fundamental researches into industrial products.

Although we are facing a large number of challenges, the promising future encourages us in this revolutionarily technology to improve our healthcare. Future wearable medical devices will undoubtedly fit human body better, moving away from bulky and rigid equipment into textiles that merge into the daily life of wearers. These textiles contain thousands of fibrous biosensors aiming at the home monitoring of human vital signs in real time. Future implanted medical devices will achieve a seamless and stable device-tissue interface to produce continuous sensing information and closed-loop treatment. The neural fibers form reliable brain-machine interfaces, helping paralyzed patients to rapidly convert neural signals into control orders for prosthetic devices or robots. These devices will not only facilitate disease prevention, or early diagnosis and treatment, but also improve the quality of patients' life and reduce medical expenses significantly. One day it will seem normal to have fibrous biomedical devices as an integral part of the body to change and improve our lives.

Conflict of Interest

The authors declare no conflict of interest.

Keywords

bioelectronics, biomedical devices, fiber, implantable, wearable

Received: April 8, 2019

Revised: May 11, 2019

Published online:

- [1] Y. Yu, H. Yuk, G. A. Parada, Y. Wu, X. Liu, C. S. Nabzdyk, *Adv. Mater.* **2019**, *31*, 1807101.
- [2] T. E. Schlaepfer, M. X. Cohen, C. Frick, M. Kosel, D. Brodesser, N. Axmacher, A. Y. Joe, M. Kreft, D. Lenartz, V. Sturm, *Neuropharmacology* **2008**, *33*, 368.
- [3] W. Zeng, L. Shu, Q. Li, S. Chen, F. Wang, X. M. Tao, *Adv. Mater.* **2014**, *26*, 5310.
- [4] A. F. Abouraddy, M. Bayindir, G. Benoit, S. D. Hart, K. Kuriki, N. Orf, O. Shapira, F. Sorin, B. Temelkuran, Y. Fink, *Nat. Mater.* **2007**, *6*, 336.
- [5] W. Yan, A. Page, T. Nguyen-Dang, Y. Qu, F. Sordo, L. Wei, F. Sorin, *Adv. Mater.* **2019**, *31*, 1802348.

- [6] N. Ashammakhi, S. Ahadian, M. A. Darabi, M. El Tahchi, J. Lee, K. Suthiwanich, A. Sheikhi, M. R. Dokmeci, R. Oklu, A. Khademhosseini, *Adv. Mater.* **2019**, *31*, 1804041.
- [7] J. Kim, A. S. Campbell, B. E.-F. de Ávila, J. Wang, *Nat. Biotechnol.* **2019**, *37*, 389.
- [8] H. Sun, Y. Zhang, J. Zhang, X. Sun, H. Peng, *Nat. Rev. Mater.* **2017**, *2*, 17023.
- [9] F. Pisanello, G. Mandelbaum, M. Pisanello, I. A. Oldenburg, L. Sileo, J. E. Markowitz, R. E. Peterson, A. Della Patria, T. M. Haynes, M. S. Emará, *Nat. Neurosci.* **2017**, *20*, 1180.
- [10] T. D. Y. Kozai, N. B. Langhals, P. R. Patel, X. Deng, H. Zhang, K. L. Smith, J. Lahann, N. A. Kotov, D. R. Kipke, *Nat. Mater.* **2012**, *11*, 1065.
- [11] A. B. Dalton, S. Collins, E. Munoz, J. M. Razal, V. H. Ebron, J. P. Ferraris, J. N. Coleman, B. G. Kim, R. H. Baughman, *Nature* **2003**, *423*, 703.
- [12] Z. Xu, C. Gao, *Nat. Commun.* **2011**, *2*, 571.
- [13] S. Shen, H. Wang, Y. Qu, K. Huang, G. Liu, Z. Chen, C. Ma, P. Shao, J. Hong, P. Lemailet, *Biomed. Opt. Express* **2019**, *10*, 571.
- [14] J. R. Raney, B. G. Compton, J. Mueller, T. J. Ober, K. Shea, J. A. Lewis, *Proc. Natl. Acad. Sci. U. S. A.* **2018**, *115*, 1198.
- [15] Q. Pi, S. Maharjan, X. Yan, X. Liu, B. Singh, A. M. van Genderen, F. Robledo-Padilla, R. Parra-Saldivar, N. Hu, W. Jia, *Adv. Mater.* **2018**, *30*, 1706913.
- [16] C. Lu, U. P. Froriep, R. A. Koppes, A. Canales, V. Caggiano, J. Selvidge, E. Bizzi, P. Anikeeva, *Adv. Funct. Mater.* **2014**, *24*, 6594.
- [17] H. Peng, *Fiber-Shaped Energy Harvesting and Storage Devices*, Springer, New York **2015**.
- [18] S. Park, Y. Guo, X. Jia, H. K. Choe, B. Grena, J. Kang, J. Park, C. Lu, A. Canales, R. Chen, *Nat. Neurosci.* **2017**, *20*, 612.
- [19] F. Meng, W. Lu, Q. Li, J. Byun, Y. Oh, T. Chou, *Adv. Mater.* **2015**, *27*, 5113.
- [20] B. Fang, L. Peng, Z. Xu, C. Gao, *ACS Nano* **2015**, *9*, 5214.
- [21] Z. Yang, H. Sun, T. Chen, L. Qiu, Y. Luo, H. Peng, *Angew. Chem., Int. Ed.* **2013**, *52*, 7545.
- [22] Y. Liu, Z. Xu, J. Zhan, P. Li, C. Gao, *Adv. Mater.* **2016**, *28*, 7941.
- [23] T. Ma, H. Gao, H. Cong, H. Yao, L. Wu, Z. Yu, S. Chen, S. Yu, *Adv. Mater.* **2018**, *30*, 1706435.
- [24] Y. Zhang, Y. Jiao, M. Liao, B. Wang, H. Peng, *Carbon* **2017**, *124*, 79.
- [25] V. A. Davis, A. N. G. Parra-Vasquez, M. J. Green, P. K. Rai, N. Behabtu, V. Prieto, R. D. Booker, J. Schmidt, E. Kesselman, W. Zhou, *Nat. Nanotechnol.* **2009**, *4*, 830.
- [26] S. Zhang, K. K. K. Koziol, I. A. Kinloch, A. H. Windle, *Small* **2008**, *4*, 1217.
- [27] N. Behabtu, C. C. Young, D. E. Tsentelovich, O. Kleinerman, X. Wang, A. W. K. Ma, E. A. Bengio, R. F. ter Waarbeek, J. J. de Jong, R. E. Hoogerwerf, *Science* **2013**, *339*, 182.
- [28] Y.-L. Li, I. A. Kinloch, A. H. Windle, *Science* **2004**, *304*, 276.
- [29] K. Jiang, Q. Li, S. Fan, *Nature* **2002**, *419*, 801.
- [30] T. Chen, L. Qiu, Z. Cai, F. Gong, Z. Yang, Z. Wang, H. Peng, *Nano Lett.* **2012**, *12*, 2568.
- [31] A. A. Kuznetsov, A. F. Fonseca, R. H. Baughman, A. A. Zakhidov, *ACS Nano* **2011**, *5*, 985.
- [32] H. Peng, X. Sun, F. Cai, X. Chen, Y. Zhu, G. Liao, D. Chen, Q. Li, Y. Lu, Y. Zhu, *Nat. Nanotechnol.* **2009**, *4*, 738.
- [33] Y. Shang, Y. Wang, S. Li, C. Hua, M. Zou, A. Cao, *Carbon* **2017**, *119*, 47.
- [34] Y. Bai, R. Zhang, X. Ye, Z. Zhu, H. Xie, B. Shen, D. Cai, B. Liu, C. Zhang, Z. Jia, *Nat. Nanotechnol.* **2018**, *13*, 589.
- [35] Y. Zhang, W. Bai, X. Cheng, J. Ren, W. Weng, P. Chen, X. Fang, Z. Zhang, H. Peng, *Angew. Chem., Int. Ed.* **2015**, *54*, 14951.
- [36] J. Ren, Q. Xu, X. Chen, W. Li, K. Guo, Y. Zhao, Q. Wang, Z. Zhang, H. Peng, Y. Li, *Adv. Mater.* **2017**, *29*, 1702713.
- [37] S. He, Y. Hu, J. Wan, Q. Gao, Y. Wang, S. Xie, L. Qiu, C. Wang, G. Zheng, B. Wang, *Carbon* **2017**, *122*, 162.
- [38] M. D. Lima, S. Fang, X. Lepró, C. Lewis, R. Ovalle-Robles, J. Carretero-González, E. Castillo-Martínez, M. E. Kozlov, J. Oh, N. Rawat, *Science* **2011**, *331*, 51.
- [39] S. Lin, H. Yuk, T. Zhang, G. A. Parada, H. Koo, C. Yu, X. Zhao, *Adv. Mater.* **2016**, *28*, 4497.
- [40] M. Akbari, A. Tamayol, S. Bagherifard, L. Serex, P. Mostafalu, N. Faramarzi, M. H. Mohammadi, A. Khademhosseini, *Adv. Healthcare Mater.* **2016**, *5*, 751.
- [41] M. Akbari, A. Tamayol, V. Laforte, N. Annabi, A. H. Najafabadi, A. Khademhosseini, D. Juncker, *Adv. Funct. Mater.* **2014**, *24*, 4060.
- [42] A. Tamayol, A. H. Najafabadi, B. Aliakbarian, E. Arab-Tehrany, M. Akbari, N. Annabi, D. Juncker, A. Khademhosseini, *Adv. Healthcare Mater.* **2015**, *4*, 2146.
- [43] Y. Yu, L. Shang, J. Guo, J. Wang, Y. Zhao, *Nat. Protoc.* **2018**, *13*, 2557.
- [44] Y. Jun, E. Kang, S. Chae, S.-H. Lee, *Lab Chip* **2014**, *14*, 2145.
- [45] E. Kang, G. S. Jeong, Y. Y. Choi, K. H. Lee, A. Khademhosseini, S.-H. Lee, *Nat. Mater.* **2011**, *10*, 877.
- [46] H. Onoe, T. Okitsu, A. Itou, M. Kato-Negishi, R. Gojo, D. Kiriya, K. Sato, S. Miura, S. Iwanaga, K. Kuribayashi-Shigetomi, *Nat. Mater.* **2013**, *12*, 584.
- [47] A. Canales, S. Park, A. Kiliyas, P. Anikeeva, *Acc. Chem. Res.* **2018**, *51*, 829.
- [48] M. Rein, V. D. Favrod, C. Hou, T. Khudiyev, A. Stolyarov, J. Cox, C.-C. Chung, C. Chhav, M. Ellis, J. Joannopoulos, *Nature* **2018**, *560*, 214.
- [49] C. Lu, S. Park, T. J. Richner, A. Derry, I. Brown, C. Hou, S. Rao, J. Kang, C. T. Moritz, Y. Fink, *Sci. Adv.* **2017**, *3*, e1600955.
- [50] R. A. Koppes, S. Park, T. Hood, X. Jia, N. A. Poorheravi, A. H. Achyuta, Y. Fink, P. Anikeeva, *Biomaterials* **2016**, *81*, 27.
- [51] Y. Khan, A. E. Ostfeld, C. M. Lochner, A. Pierre, A. C. Arias, *Adv. Mater.* **2016**, *28*, 4373.
- [52] H. Lee, C. Song, Y. S. Hong, M. S. Kim, H. R. Cho, T. Kang, K. Shin, S. H. Choi, T. Hyeon, D.-H. Kim, *Sci. Adv.* **2017**, *3*, e1601314.
- [53] C. S. Wood, M. R. Thomas, J. Budd, T. P. Mashamba-Thompson, K. Herbst, D. Pillay, R. W. Peeling, A. M. Johnson, R. A. McKendry, M. M. Stevens, *Nature* **2019**, *566*, 467.
- [54] A. K. Yetisen, J. L. Martinez-hurtado, A. Khademhosseini, *Adv. Mater.* **2018**, *30*, 1706910.
- [55] F. Zhao, Y. Zhao, H. Zhao, L. T. Qu, *Angew. Chem., Int. Ed.* **2015**, *54*, 14951.
- [56] T. Yamada, Y. Hayamizu, Y. Yamamoto, Y. Yornogida, A. Izadi-Najafabadi, D. N. Futaba, K. Hata, *Nat. Nanotechnol.* **2011**, *6*, 296.
- [57] L. Lu, Y. Zhou, J. Pan, T. Chen, Y. Hu, G. Zheng, K. Dai, C. Liu, C. Shen, X. Sun, H. Peng, *ACS Appl. Mater. Interfaces* **2019**, *11*, 4345.
- [58] Z. Wang, Y. Huang, J. Sun, Y. Huang, H. Hu, R. Jiang, W. Gai, G. Li, C. Zhi, *ACS Appl. Mater. Interfaces* **2016**, *8*, 24837.
- [59] S. Lee, S. Shin, S. Lee, J. Seo, J. Lee, S. Son, H. J. Cho, H. Algadi, S. Al-Sayari, D. E. Kim, *Adv. Funct. Mater.* **2015**, *25*, 3114.
- [60] Y. Li, B. Zhou, G. Zheng, X. Liu, T. Li, C. Yan, C. Cheng, K. Dai, C. Liu, C. Shen, *J. Mater. Chem. C* **2018**, *6*, 2258.
- [61] A. Frutiger, J. T. Muth, D. M. Vogt, Y. Mengüç, A. Campo, A. D. Valentine, C. J. Walsh, J. A. Lewis, *Adv. Mater.* **2015**, *27*, 2440.
- [62] J. Lee, H. Kwon, J. Seo, S. Shin, J. H. Koo, C. Pang, S. Son, J. H. Kim, Y. H. Jang, D. E. Kim, *Adv. Mater.* **2015**, *27*, 2433.
- [63] X. Wang, J. Zhou, J. Song, J. Liu, N. Xu, Z. L. Wang, *Nano Lett.* **2006**, *6*, 2768.
- [64] H. Gullapalli, V. S. M. Vemuru, A. Kumar, A. Botello-Mendez, R. Vajtai, M. Terrones, S. Nagarajaiah, P. M. Ajayan, *Small* **2010**, *6*, 1641.
- [65] E. Nilsson, A. Lund, C. Jonasson, C. Johansson, B. Hagström, *Sens. Actuators, A* **2013**, *201*, 477.

- [66] K. Dong, J. Deng, Y. Zi, Y. Wang, C. Xu, H. Zou, W. Ding, Y. Dai, B. Gu, B. Sun, *Adv. Mater.* **2017**, *29*, 1702648.
- [67] K. Dong, Z. Wu, J. Deng, A. C. Wang, H. Zou, C. Chen, D. Hu, B. Gu, B. Sun, Z. L. Wang, *Adv. Mater.* **2018**, *30*, 1804944.
- [68] A. Tamayol, M. Akbari, Y. Zilberman, M. Comotto, E. Lesha, L. Serex, S. Bagherifard, Y. Chen, G. Fu, S. K. Ameri, *Adv. Healthcare Mater.* **2016**, *5*, 711.
- [69] W. Gao, S. Emaminejad, H. Y. Y. Nyein, S. Challa, K. Chen, A. Peck, H. M. Fahad, H. Ota, H. Shiraki, D. Kiriya, *Nature* **2016**, *529*, 509.
- [70] L. Wang, L. Wang, Y. Zhang, J. Pan, S. Li, X. Sun, B. Zhang, H. Peng, *Adv. Funct. Mater.* **2018**, *28*, 1804456.
- [71] H. Lee, T. K. Choi, Y. B. Lee, H. R. Cho, R. Ghaffari, L. Wang, H. J. Choi, T. D. Chung, N. Lu, T. Hyeon, *Nat. Nanotechnol.* **2016**, *11*, 566.
- [72] M. Amjadi, S. Sheykhsari, B. J. Nelson, M. Sitti, *Adv. Mater.* **2018**, *30*, 1704530.
- [73] P. Mostafalu, G. Kiaee, G. Giatsidis, A. Khalilpour, M. Nabavinia, M. R. Dokmeci, S. Sonkusale, D. P. Orgill, A. Tamayol, A. Khademhosseini, *Adv. Funct. Mater.* **2017**, *27*, 1702399.
- [74] M. Nazari, M. Rubio-Martinez, G. Tobias, J. P. Barrio, R. Babarao, F. Nazari, K. Konstas, B. W. Muir, S. F. Collins, A. J. Hill, *Adv. Funct. Mater.* **2016**, *26*, 3244.
- [75] T. Someya, Z. Bao, G. G. Malliaras, *Nature* **2016**, *540*, 379.
- [76] M. H. Yacoub, C. McLeod, *Nat. Rev. Cardiol.* **2018**, *15*, 770.
- [77] C. M. Boutry, L. Beker, Y. Kaizawa, C. Vassos, H. Tran, A. C. Hinckley, R. Pfattner, S. Niu, J. Li, J. Claverie, *Nat. Biomed. Eng.* **2019**, *3*, 47.
- [78] L. Zhang, F. Liu, X. Sun, G. Wei, Y. Tian, Z. Liu, R. Huang, Y. Yu, H. Peng, *Anal. Chem.* **2017**, *89*, 1831.
- [79] L. Liu, F. Zhao, W. Liu, T. Zhu, J. Z. H. Zhang, C. Chen, Z. Dai, H. Peng, J. Huang, Q. Hu, *Angew. Chem., Int. Ed.* **2017**, *129*, 10607.
- [80] M. Choi, M. Humar, S. Kim, S. Yun, *Adv. Mater.* **2015**, *27*, 4081.
- [81] A. K. Yetisen, N. Jiang, A. Fallahi, Y. Montelongo, G. U. Ruiz-Esparza, A. Tamayol, Y. S. Zhang, I. Mahmood, S. Yang, K. S. Kim, *Adv. Mater.* **2017**, *29*, 1606380.
- [82] O. Vermesh, A. Aalipour, T. J. Ge, Y. Saenz, Y. Guo, I. S. Alam, S. Park, C. N. Adelson, Y. Mitsutake, J. Vilches-Moure, *Nat. Biomed. Eng.* **2018**, *2*, 696.
- [83] X. Yu, H. Wang, X. Ning, R. Sun, H. Albadawi, M. Salomao, A. C. Silva, Y. Yu, L. Tian, A. Koh, *Nat. Biomed. Eng.* **2018**, *2*, 165.
- [84] D. An, Y. Ji, A. Chiu, Y. Lu, W. Song, L. Zhai, L. Qi, D. Luo, M. Ma, *Biomaterials* **2015**, *37*, 40.
- [85] D. An, A. Chiu, J. A. Flanders, W. Song, D. Shou, Y.-C. Lu, L. G. Grunnet, L. Winkel, C. Ingvorsen, N. S. Christophersen, *Proc. Natl. Acad. Sci. U. S. A.* **2018**, *115*, E263.
- [86] A. R. Pepper, B. Gala-Lopez, R. Pawlick, S. Merani, T. Kin, A. M. J. Shapiro, *Nat. Biotechnol.* **2015**, *33*, 518.
- [87] T. Desai, L. D. Shea, *Nat. Rev. Drug Discovery* **2017**, *16*, 338.
- [88] J. Shi, Y. Fang, *Adv. Mater.* **2018**, 1804895.
- [89] R. Chen, A. Canales, P. Anikeeva, *Nat. Rev. Mater.* **2017**, *2*, 16093.
- [90] K. Wang, C. L. Frewin, D. Esrafilzadeh, C. Yu, C. Wang, J. J. Pancrazio, M. Romero-Ortega, R. Jalili, G. Wallace, *Adv. Mater.* **2019**, *31*, 1805867.
- [91] F. Vitale, S. R. Summerson, B. Aazhang, C. Kemere, M. Pasquali, *ACS Nano* **2015**, *9*, 4465.
- [92] A. Canales, X. Jia, U. P. Fropie, R. A. Koppes, C. M. Tringides, J. Selvidge, C. Lu, C. Hou, L. Wei, Y. Fink, *Nat. Biotechnol.* **2015**, *33*, 277.
- [93] C. Dagdeviren, K. B. Ramadi, P. Joe, K. Spencer, H. N. Schwerdt, H. Shimazu, S. Delcasso, K. Amemori, C. Nunez-Lopez, A. M. Graybiel, *Sci. Transl. Med.* **2018**, *10*, eaan2742.
- [94] X. Yang, T. Zhou, T. J. ZWang, G. Hong, Y. Zhao, R. D. Viveros, T. Fu, T. Gao, C. M. Lieber, *Nat. Mater.* **2019**, *18*, 510.
- [95] Y. Zhang, Y. Jiao, L. Lu, L. Wang, T. Chen, H. Peng, *Angew. Chem., Int. Ed.* **2017**, *56*, 13741.
- [96] J. Ren, Y. Zhang, W. Bai, X. Chen, Z. Zhang, X. Fang, W. Weng, Y. Wang, H. Peng, *Angew. Chem., Int. Ed.* **2014**, *126*, 7998.
- [97] B. Shi, Z. Li, Y. Fan, *Adv. Mater.* **2018**, *30*, 1801511.